RSC Advances

PAPER

View Article Online
View Journal | View Issue



Cite this: *RSC Adv.*, 2022, **12**, 1121

# The effect of $Fe^{3+}$ ions on the electrochemical behaviour of ocean manganese nodule reduction leaching in sulphuric acid solution

Jinxing Kang, Yayun Wang and Yunfei Qiu *

The effect of $Fe^{3+}$ ions on the ocean manganese nodule reductive leaching in imitated sulphuric acid solutions was investigated. This work is presented in two courses, including the influence of $Fe^{3+}$ ions on valuable metal extraction and the electrochemical reductive dissolution of manganese nodules. The results show that the beneficial effects of $Fe^{3+}$ ion can be interpreted based on two aspects: the first is the acceleration caused by the active transformation of $Fe^{3+}/Fe^{2+}$ pair, and the second is the hydrogen ion buffer action generated by $Fe^{3+}$ ion hydrolysis on the surface. On one side, $Fe^{3+}$ ion could lessen the hydrogen consumption happening at the interface layer of the nodule supported by the leaching test and cyclic voltammetry results. On the other side, $Fe^{3+}$ ions could be converted into $Fe^{2+}$ ions and then preferentially reduce manganese oxide leading to an acceleration of the charge transfer reaction of the manganese nodule based on cyclic voltammetry, polarization, and impedance analysis results. The reduction leaching of manganese nodules in sulphuric acid solution is mainly controlled by the electrochemical interface reduction corresponding to manganese oxide dissolution, and the active conversion of the $Fe^{3+}/Fe^{2+}$ couple affects the dissolution of high valence manganese oxide.

Received 17th November 2021
Accepted 16th December 2021

DOI: 10.1039/d1ra08440b

rsc.li/rsc-advances



## 1. Introduction

Ocean manganese nodules, also known as ocean polymetallic nodules and ocean ferromanganese nodules, are complex polymetallic iron–manganese ores that are rich in manganese, nickel, cobalt, copper, iron, and other valuable metals. It has been considered the most economically valuable oceanic mineral resource.[1–3] Generally, a manganese nodule is an aggregate of a shell of iron and manganese oxides wrapping a core of clay minerals. With regard to the shell of the manganese nodule, manganese minerals are usually present in vernadite, todorokite, birnessite, and buserite, and iron mainly forms oxides and hydroxides of ferric iron. It has been reported that manganese oxides and iron oxides present in the form of poorly crystalline states are nearly disseminated associations.[4–7] Moreover, studies have suggested that the extraction of Ni, Co, and Cu from manganese nodules is much related to the destruction of the structure of Fe–Mn oxides as these metals are presenting specialistic and preferential adsorption of ferromanganese oxides.[8–10] In other words, the transformation and separation of the Fe–Mn oxides are a necessary precondition for the recoveries of valuable metals from manganese nodules.

Research on the beneficiation and metallurgy process of manganese nodules are conducted in many countries throughout the world since the early 1950s. Now, there have been reports on some representative processing methods, such as reduction roasting-ammonia leaching,[11] cuprous ion catalytic reduction-ammoniacal leaching,[12] reduction acid leaching in $H_2SO_4$ or HCl system,[13,14] rusting-leaching process,[15] and bioleaching.[16] A critical review of the literature, especially in terms of energy consumption, carbon emission, and selective extraction, indicates that the reductive leaching of manganese nodules in the sulphuric acid system is a relatively promising and inexpensive approach.

In regard to the metal extraction from manganese nodules using sulphuric acid solution, it has been profusely investigated the applications of reduction technologies and reducing agents. At present, many reductive methods and agents have been reported for their feasibility and potential, such as the application of pyrite, sulfur dioxide, hydrogen sulphide, ferrous ion, organic wastewater, and glucose as reducing solvents for polymetallic nodules in the sulphuric acid system.[17–20] From these methods, the efficient extraction of multiple metals from manganese nodules is largely depended on the reducing leaching of Mn–Fe oxides, that is to say, Mn–Fe oxides of manganese nodule dissolution in the solution is a precondition for the metal extraction from manganese nodule in sulphuric acid solution.

So far, many studies have reported the dissolution performance of Mn–Fe oxides from manganese nodules, and some studies have investigated the interface reaction of Mn-oxides from manganese nodules.[21–23] Fe-oxides, as a basic mineral in manganese nodules, could be dissolved to produce $Fe^{3+}$ ions in the solution, affecting the process of manganese nodule

*China ENFI Engineering Co., Ltd, China Minmetal, Beijing 100038, China*

reductive leaching in sulphuric acid solution. However, the performance of $Fe^{3+}$ ions on the reductive leaching of manganese nodules in sulphuric acid solution is considerably less-studied. As is well known, the Mn–Fe oxide reductive dissolution of manganese nodule in sulphuric acid solution is an electrochemical corrosion process, related to the transformation of substances between the ore electrode and dissolved solution. Hence, the electrochemical behaviour function analysis of $Fe^{3+}$ ion-effect on the reduction of Mn–Fe oxides from manganese nodules may be an invaluable topic for investigation.

The aim of this work was to investigate the effect of $Fe^{3+}$ ions on the reduction leaching of manganese nodule in sulphuric acid solution. The influence of $Fe^{3+}$ ions on the extraction of Ni, Co, Cu, Mn, and Fe was evaluated using simulated dissolution tests in sulphuric acid systems. The reductive electrochemical corrosion processes of manganese nodules in the presence and absence of $Fe^{3+}$ ion electrolysis solution, were investigated using multiple electrochemical methods. The effect of $Fe^{3+}$ ions on the dissolution process of manganese nodules was discussed in the context of $Fe^{3+}$ ion-sulphuric acid system.

## 2. Materials and methods

### 2.1 Materials and solvent system

The ocean manganese nodules were obtained from the China pioneer area of the eastern Pacific ocean. The nodules with a specific surface area of 8.8 $m^2\ g^{-1}$ were air-dried, crushed, and ground to 74 μm size before use. The main chemical composition analysis results of nodules are shown in Table 1. Fig. 1 presents the XRD patterns of the nodule. The main metals in nodules include manganese, nickel, copper, cobalt, and iron. Manganese and iron were mainly present in the form of high valence oxides in the ferromanganese nodule, and nickel, copper, and cobalt ions formed characteristic adsorption dispersed in the lattice gape of the Mn–Fe oxides.

The solvent systems were prepared using $Fe^{3+}$ ion-free and $Fe^{3+}$ ion-containing diluted sulphuric acid solution. The control group was $Fe^{3+}$ ion-free diluted sulphuric acid solution. A selected mass of ferric sulfate ($Fe_2(SO_4)_3$) was dissolved in diluted sulphuric acid solution containing $Fe^{3+}$ ion-containing solution. A solution of 10% $H_2SO_4$ was used to adjust the pH of the solution. Analytical reagents were used in this work.

### 2.2 Metal extraction performance tests

The metal extraction tests on manganese nodules were performed in a simulated electrolytic leaching system connected to an electrochemical workstation (CHI1140C, CH Instruments, USA). The schematic of the simulated leaching of manganese nodules is shown in Fig. 2. A three-electrode system was used, using a Pt plate (1.0 $cm^2$) as a counter electrode, a standard calomel electrode (SCE) as a reference electrode (0.24 V *vs.* the standard hydrogen electrode (SHE)), and a loaded ferromanganese nodule powder on a graphite felt as a working electrode. The preparation of ferromanganese nodule electrode involved depositing a thin layer of the nodule ink over a graphite felt (1.0 $cm^2$). The nodule grain ink was prepared by mixing the manganese nodule (90 wt%) and, polytetrafluroethylene (10 wt%) in *N*-methyl-2-pyrrolidone (the mass of the nodule was fixed at 0.2 g).[24] The leaching of metals from manganese nodule was measured by electrolyzing manganese nodules electrode in a simulated dissolution solution. Simulated leaching solutions were prepared as $Fe^{3+}$ ion-free and $Fe^{3+}$ ion-containing dilute sulphuric acid solutions. The input voltage of the manganese nodule working electrode was at −1.0 V, and 200 mL of the dissolution solution was used for each test. The influences of leaching characteristic on the pH value and $Fe^{3+}$ ion concentration were measured from Mn, Ni, Co, Cu, and Fe extraction efficiencies calculated from the raw material content in lixiviums at a stated time. A water bath kettle was used to maintain the leaching simulation temperature at 25 °C, and a magnetic rotor was used for agitating the leaching solution. The pH of the leaching solution was buffered using dilute sulphuric acid and potassium hydroxide solution. The dissolved Mn, Ni, Co, Cu, and Fe concentrations in the obtained solutions were determined from ICP-OES analysis (Agilent 5800 ICP-OES, Agilent, Germany).

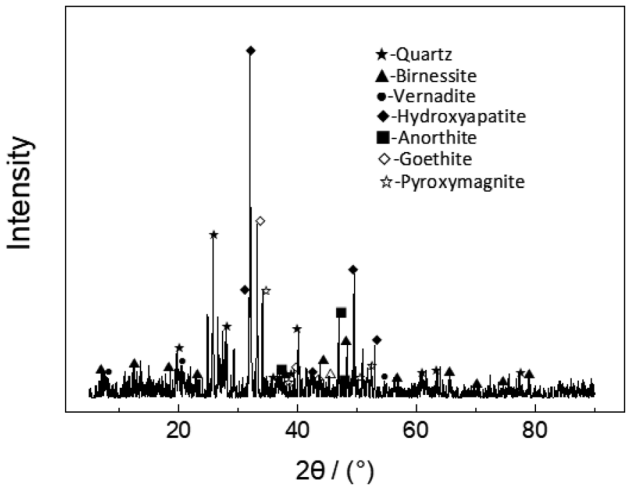


Fig. 1 XRD pattern of the manganese nodule.

Table 1 Main chemical compositions of the ferromanganese nodule (%, mass fraction)

| Element | Ni | Cu | Co | $SiO_2$ | $Na_2O$ | $K_2O$ |
|---|---|---|---|---|---|---|
| wt% | 1.63 | 1.37 | 0.20 | 22.45 | 0.32 | 3.44 |
| Element | Mn | Fe | S | $Al_2O_3$ | CaO | $TiO_2$ |
| wt% | 22.15 | 11.67 | 0.31 | 7.82 | 3.12 | 1.03 |

### 2.3 Electrochemical measurements

Electrochemical measurements were performed in a typical electrochemical cell with three electrodes on a CHI1140C microcomputer-based electrochemical system, the electrodes and electrolytes were prepared in line with the description from Section 2.2. The three electrodes were immersed in the $Fe^{3+}$ ion-free or $Fe^{3+}$ ion-containing leaching solution for 20 min and the

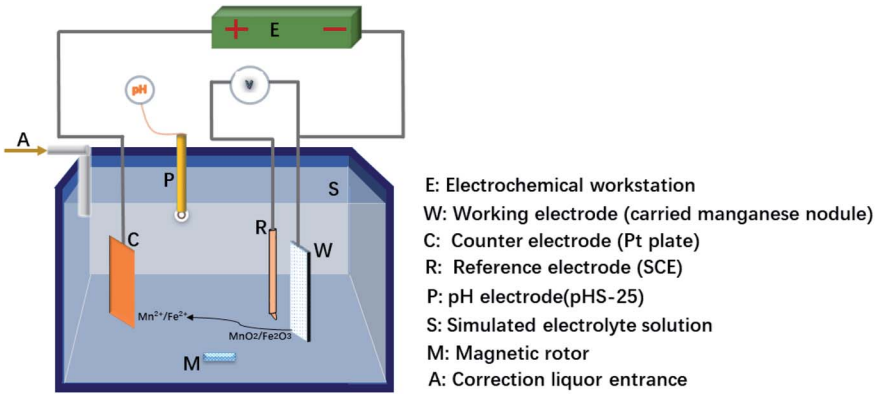


Fig. 2 Schematic of the simulated leaching measurement of manganese nodule.

scan was started. The cyclic voltammetry evaluations were performed by sweeping from −0.6 V (positive-going potential scan) to 1.2 V (negative-going potential scan) and back to the starting potential with a sweep rate of 25 mV $s^{-1}$. Potentiodynamic polarization curves were obtained from −0.6 to 1.5 V with a scanning rate of 5 mV $s^{-1}$. Impedance spectra were generated at the open circuit potential (OPC) by using a sine wave voltage amplitude of 5 mV during the frequency region from 0.01 to $10^5$ Hz. The EIS (electrochemical impedance spectroscopy) data were presented in Nyquist plots and analysis using Zview 2.0 software. The temperature of all electrochemical measurements was kept at 25 °C. All the potentials shown in this work were relative to SCE.

## 3. Results and discussion

### 3.1 Effect of $Fe^{3+}$ ion on metal extraction

**3.1.1 Metal extraction response of leaching system.** The influence of $Fe^{3+}$ ion on the extraction of metals from manganese nodules in the presence and absence of $Fe^{3+}$ ion solutions, as determined from the extraction ratios of Mn, Ni, Cu, Co, and Fe, is presented in Fig. 3. The dissolution efficiencies of Ni, Cu, Co, and Mn positively responded to the presence of $Fe^{3+}$ ions, and the main metals Ni, Cu, and Co showed extractions similar to the leaching tendency of Mn dissolution under the test conditions. Combined with previous studies,[25,26] it is reasonable to adopt Mn extraction efficiency to discuss the effect of $Fe^{3+}$ ions on the reductive leaching of manganese nodules in sulphuric acid solution.

**3.1.2 Response of pH and $Fe^{3+}$ ion concentration.** Fig. 4 shows Mn dissolution from the manganese nodule under different pH values, assisted with or without $Fe^{3+}$ ions in the initial leaching solution. The Mn dissolution of manganese nodule responds positively to $Fe^{3+}$ ion concentration and acidity under the test conditions, and $Fe^{3+}$ ions affect the Mn leaching that correlates with the acidity of the bath solution (Fig. 4).

A higher initial $Fe^{3+}$ ion concentration leads to a faster leaching rate of Mn, illustrating that $Fe^{3+}$ ion could accelerate the reduction of $Mn^{4+}$ to $Mn^{2+}$ as shown in Fig. 4(a). With the usage of 0.1 g $L^{-1}$ $Fe^{3+}$ ion in the initial solution, Mn leaching rate increased nearly 10% with reference to the control at pH 1.8, and there was about 18% increase in the Mn leaching rate when $Fe^{3+}$ ion concentration was over 1.0 g $L^{-1}$, indicating that the effect of $Fe^{3+}$ ion on Mn leaching, caused by $Fe^{3+}$ ion concentration increased, was shown to a limited extent.

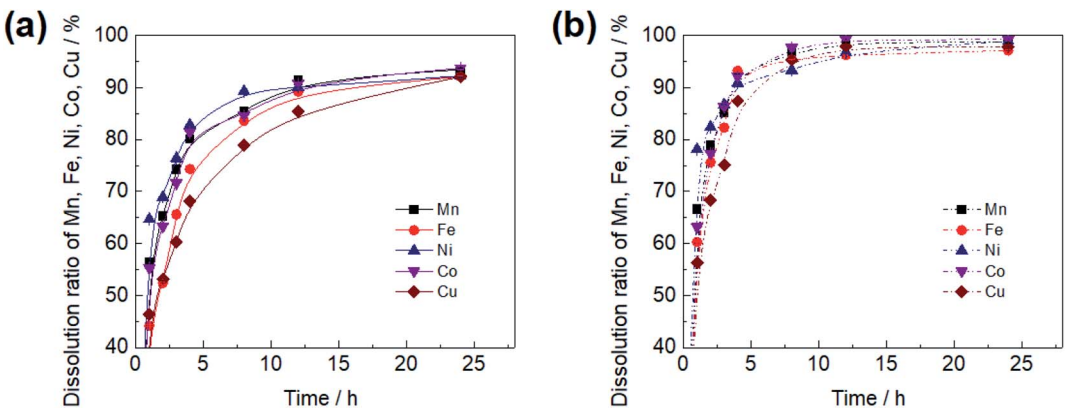


Fig. 3 Effects of $Fe^{3+}$ ions on Mn, Fe, Ni, Co, and Cu extraction ratios from the manganese nodule: (a) the initial $Fe^{3+}$ iron-free solution, pH 1.8; (b) $Fe^{3+}$ ion-containing solution, initial $Fe^{3+}$ ion concentration of 1.0 g $L^{-1}$, pH 1.8.

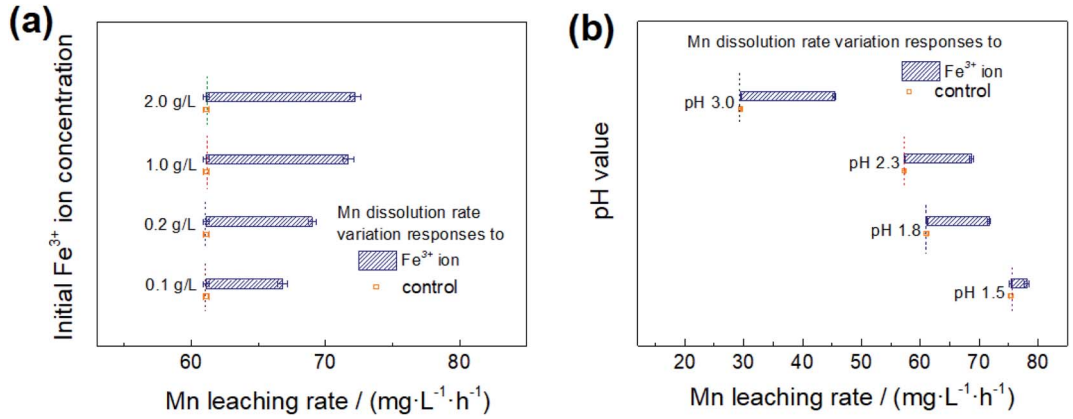


Fig. 4 Effects of $Fe^{3+}$ ion concentration and pH value on the Mn-extraction rate from manganese nodules: (a) response to $Fe^{3+}$ ion concentration, $Fe^{3+}$ ion-free solution as control, pH 1.8; (b) response to pH, $Fe^{3+}$ iron-free solution as control, initial $Fe^{3+}$ ion concentration of 1.0 g $L^{-1}$ as the $Fe^{3+}$ ion-containing solution.

A high-level of acidity corresponds to a high leaching rate of Mn dissolution in non-$Fe^{3+}$ ion and with $Fe^{3+}$ ion solutions, as the Mn reductive dissolution of manganese nodule is a reaction involving hydrogen consumption (Fig. 4(b)). Hence, the Mn extraction rate is nearly two and a half times at pH 1.5 as compared to pH 3.0 in $Fe^{3+}$ion-containing an initial solution, as well as $Fe^{3+}$ ion-free solution. With acidity decreasing, the effect of the presence of $Fe^{3+}$ ion increased, and Mn leaching rate showed 15.8 mg $(L\ h)^{-1}$ increase at pH 3.0 and 2.7 mg $(L\ h)^{-1}$ at pH 1.5 relative to the control group, suggesting that $Fe^{3+}$ ion hydrolysis on the surface of manganese nodules, facilitating the conversion of free hydrogen.[27]

According to the leaching results shown in Fig. 4, $Fe^{3+}$ ions, and acidity should have a synergistic effect on Mn-leaching efficiency. Therefore, it could be concluded that the preferred acidity of pH 1.8 and $Fe^{3+}$ ion concentration of 1.0 g $L^{-1}$ as an appropriate influence factor for the metal extraction of the manganese nodule and electrochemical measurements.

### 3.2 The effect of $Fe^{3+}$ ions on the electrochemical behaviour

**3.2.1 Cyclic voltammetry analysis.** Fig. 5 shows cyclic voltammograms of manganese nodules in different simulated solutions. The dissolution of manganese nodules in sulphuric acid solution principally presents a result of the redox reaction of Mn-and-Fe oxides, as shown in Fig. 5(a)–(c). The pairs of redox currents corresponding to $MnO_2/Mn(OH)_2$, $Fe^{3+}/Fe^{2+}$, and $MnO_2/Mn^{2+}$ emerge between −0.3 and 0.1 V, 0.3 and 0.8 V, and 0.8 and 1.2 V (*vs.* SCE), respectively, illustrating that the dissolution of the nodule is mainly related to the reductive conversion of high valence manganese and iron oxides in sulphuric acid systems. Acidity and $Fe^{3+}$ ion have significant influence on the Mn–Fe oxides reduction.

In the $Fe^{3+}$ ion-free solutions, the conversion of $MnO_2$ to $Mn^{2+}$ shows an evident current response, stronger than other reduction responses, indicating that the dissolution of manganese nodules is mainly concerned with a reduction of high valence Mn-oxides. The current density of the reduction peak of $MnO_2/Mn^{2+}$ is higher at pH 1.5 than at pH 1.8, and the potential positively moves closer to the balance potential of $MnO_2/Mn^{2+}$ with acidity increasing to pH 1.5, suggesting that the increase in acidity leads to a high reducing rate of the nodule electrode. Moreover, an increment in the solution acidity causes a promotion on the reduction of $Fe^{3+}/Fe^{2+}$, indicating that the increased hydrogen ion concentration could facilitate the dissolution of the nodule Fe-oxides.

$Fe^{3+}$ ion has a significant effect on the reduction leaching of manganese nodules in sulphuric acid leaching solution based on optimization to the conversions of iron species. The closed area of the cyclic voltammetry curve increased when 1.0 g $L^{-1}$ $Fe^{3+}$ ion was added to the control solution, suggesting a boost in the transformation between the manganese nodule and solvent solution. With the addition of $Fe^{3+}$ ions, the reduction leaching of manganese nodules lowers the influence of acidity of the solution as the hydrolysis of $Fe^{3+}$ ions generates free hydrogen ions on the surface of the nodule, well coinciding with the leaching test results. When the $Fe^{3+}$ ion-containing solution was of pH value 1.8, the reduction current density response to $Fe^{3+}/Fe^{2+}$ had the strongest intensity compared to those at other pH value solutions, while the reductive response of $MnO_2/Mn^{2+}$ was weaker than pH 1.5 solution, suggesting that $Fe^{3+}$ ions, similar to high valence Mn-oxides, as an electron acceptor, could compete with electron from $Mn^{4+}$-oxides on the solid–liquid interface, and an electron donor preferred the reductive transformation of $MnO_2/Mn^{2+}$ under an appropriated acidity. The course of the metal extraction from the manganese nodule could be listed as follows:[24,28,29]

$$MnO_2 + 4H^+ + 2e \rightarrow Mn^{2+} + 2H_2O\ E^0 = 0.99\ V \quad (1)$$

$$MnO_2 + 2H_2O + 2e \rightarrow Mn(OH)_2 + 2OH^-\ E^0 = -0.29\ V \quad (2)$$

$$Fe^{3+} + e \rightarrow Fe^{2+}\ E^0 = 0.53\ V \quad (3)$$

$$Me(Ni, Cu, Co)O + 2H^+ \rightarrow Me(Ni, Cu, Co)^{2+} + H_2O \quad (4)$$

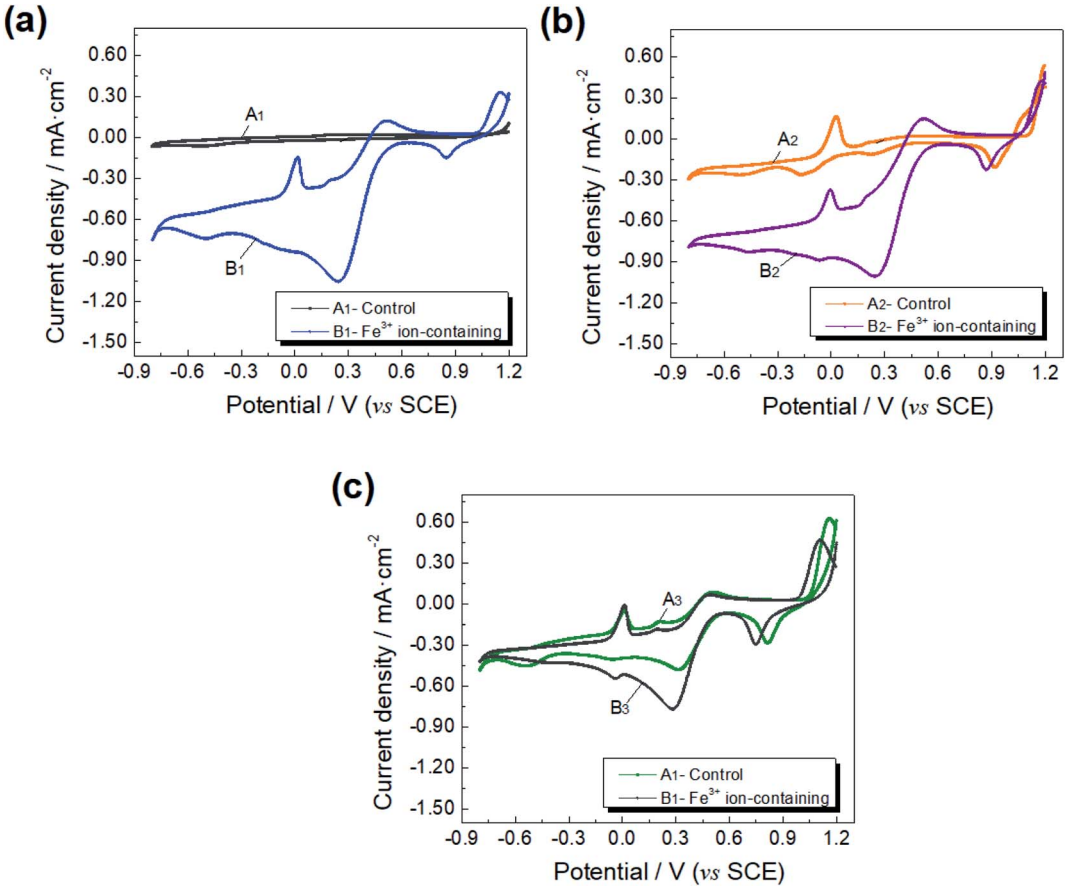


Fig. 5 Plots of cyclic voltammogram analysis of the manganese nodule in various solutions: 25 °C, 25 mV s$^{-1}$, −0.6–1.2 V (*vs.* SCE), (a)–(c) solutions, (a) pH 2.3, non $Fe^{3+}$ ion as a control, $Fe^{3+}$ ion concentration of 1.0 g L$^{-1}$ as $Fe^{3+}$ ion-containing; (a) pH 1.8, non $Fe^{3+}$ ion as a control, $Fe^{3+}$ ion concentration of 1.0 g L$^{-1}$ as $Fe^{3+}$ ion-containing; (c) pH 1.5, non $Fe^{3+}$ ion as a control, $Fe^{3+}$ ion concentration of 1.0 g L$^{-1}$ as $Fe^{3+}$ ion-containing.

**3.2.2 Polarization curve analysis.** Fig. 6 presents potentiodynamic polarization curves of the manganese nodule in various solutions. With the presence of $Fe^{3+}$ ions in the imitated leaching solution, corrosion current density increased, indicating that $Fe^{3+}$ ion facilitates the dissolution rate of manganese nodule as shown in Fig. 6 and Table 2. There is a 0.07 V negative movement of the corrosion potential appearing at 0.84 V and a 93% increase of corrosion current density if 1.0 g L$^{-1}$ $Fe^{3+}$ ions are added to the non-iron sulphuric acid solution when using negative-going scan (1.5 to −0.6 V) (Fig. 6(a)). When the curves were measured by positive-going scan (−0.6 to 1.5 V) (*vs.* SCE) (Fig. 6(b)), the corrosion potential of the manganese appear at 0.61 V in the presence of $Fe^{3+}$ ions, which was positively moved by 0.17 V in relation to the absence of $Fe^{3+}$ ion, and the self-corrosion current density was $3.23 \times 10^{-3}$ mA cm$^{-2}$ in $Fe^{3+}$ ion-containing solution, which has about six-fold increase than that of the control solution. Fig. 6(c) shows the cathodic and anodic current densities of the nodule increasing during the polarized region in the $Fe^{3+}$ ion-containing solution relative to the control group. These results illustrate that the contribution of $Fe^{3+}/Fe^{2+}$ transformation accelerates the dissolution of Mn–Fe oxides from manganese nodules, and $Fe^{3+}$ ions, on the surface of the manganese nodule, are transformed to $Fe^{2+}$ ions and then oxidized by $Mn^{4+}$-oxide leading to a preferential dissolution of $Mn^{4+}$-oxide.

**3.2.3 Alternating-current impedance analysis.** Fig. 7 show Nyquist plots (a), Bode plots (b), and the fitting equivalent circuit for the manganese nodule electrodes in $Fe^{3+}$ ion-free and $Fe^{3+}$ ion-containing solutions. Table 3 shows the fitting results for impedance data used as a simple equivalent circuit of $R_{sol}(R_{act}CPE_1)$. $R_{sol}$ and $R_{act}$ corresponded to the solution resistance values and the charge transfer resistance, respectively, $CPE_1$ represent the double-layer capacitance between the electrode and electrode interface, and $\eta$ reflected the dispersion index of $CPE_1$.

$Fe^{3+}$ ions accelerate the electron transmission during manganese nodule reductive leaching. Nyquist curves for nodules present as almost semicircles, and Bode curves show one characteristic parameters in $Fe^{3+}$ ion or non $Fe^{3+}$ ion sulphuric acid solutions (Fig. 7), indicating that the reductive dissolution of manganese nodules in the sulphuric acid system is controlled by the interfacial chemical reaction. Using 1.0 g L$^{-1}$ $Fe^{3+}$ ion in the sulphuric acid solution, it leads to the maximum peak of phase angle moving to high frequency, illustrating that $Fe^{3+}$ ions could shorten the time for electron

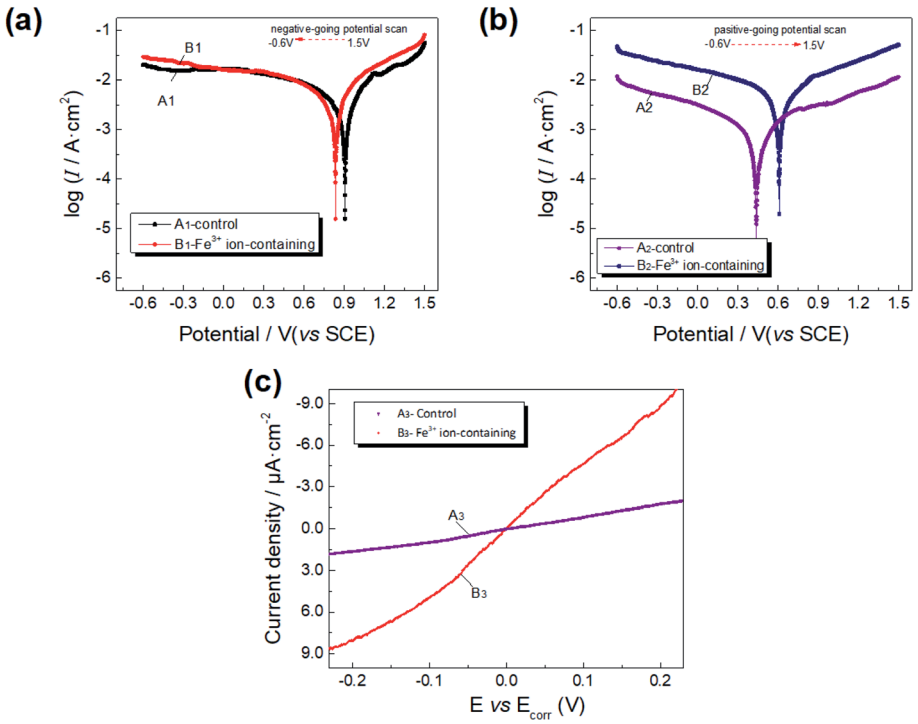


Fig. 6 Plots of polarization analysis of manganese nodules in various solutions: 25 °C, 5 mV $s^{-1}$, −0.6–1.5 V (*vs.* SCE), (a) negative-going scan, pH 1.8, non $Fe^{3+}$ ions as a control, $Fe^{3+}$ ion concentration of 1.0 g $L^{-1}$ as $Fe^{3+}$ ion-containing; (b) positive-going scan, pH 1.8, non $Fe^{3+}$ ions as a control, $Fe^{3+}$ ion concentration of 1.0 g $L^{-1}$ as $Fe^{3+}$ ion-containing; (c) pH 1.8, non $Fe^{3+}$ ions as a control, $Fe^{3+}$ ion concentration of 1.0 g $L^{-1}$ as $Fe^{3+}$ ion-containing.

travel through the interfacial electric double-layer (when frequency: $f \geq 10^3$ Hz). Furthermore, the addition of 1.0 g $L^{-1}$ $Fe^{3+}$ ions to the control solution generates an approximately 23.9% decrease in the charge-transfer resistance of manganese nodules.

### 3.3 Effect of $Fe^{3+}$ ions on the reduction of manganese nodules

The reductive dissolution of ocean ferromanganese nodules in sulphuric acid solution, is a multi-component dissolution process of iron- and manganese-oxides reduction combined with acid dissolution of metal oxides, which remarkably rely on the reductive conversion of Fe–Mn oxides. The reductive leaching of ferromanganese nodule in the sulphuric acid system is primarily concerned with reduction leaching of Fe–Mn oxides and acid dissolution of Me(Ni, Co, Cu) metal, could be expressed as:

$$MnO_2 + 4H^+ + 2e \xrightarrow{Fe^{3+}/Fe^{2+}\ ion} Mn^{2+} + 2H_2O \quad E^0 = 0.99\ V \quad (5)$$

$$Fe^{3+} + e \overset{Fe^{3+}\ ion}{\leftrightarrow} Fe^{2+} \quad E^0 = 0.53\ V \quad (6)$$

$$Me(Ni, Cu, Co)O + 2H^+ \rightarrow Me(Ni, Cu, Co)^{2+} + H_2O \quad (7)$$

In accordance with the earlier finding, $Fe^{3+}$ ions have positive effects on the reductive leaching of manganese nodules under the test conditions. The leaching performance of manganese nodules and cyclic voltammetry analysis suggests that $Fe^{3+}$ ions could lessen the hydrogen consumption happening at the interfacial layer.[30] $Fe^{3+}$ ions could be converted into $Fe^{2+}$ ions, which preferred to reduce high valence manganese oxides on the nodule surface according to the results of cyclic voltammetry and polarization results.[31] The impedance test results indicate that $Fe^{3+}$ ions accelerate the charge transfer reaction of manganese nodule reduction.[32] Combining the

Table 2 Analysis results of corrosion potential and corrosion current density for manganese nodule electrodes in various solutions

| Scanning direction | Simulated solution | Corrosion potential (V) | Corrosion current density (mA $cm^{-2}$) |
|---|---|---|---|
| Negative-going scanning (1.5 to −0.6 V (*vs.* SCE)) | $Fe^{3+}$ ion-containing | 0.836 | $3.75 \times 10^{-3}$ |
| | Control | 0.907 | $1.94 \times 10^{-3}$ |
| Positive-going scanning (−0.6 to 1.5 V (*vs.* SCE)) | $Fe^{3+}$ ion-containing | 0.610 | $3.23 \times 10^{-3}$ |
| | Control | 0.438 | $0.48 \times 10^{-3}$ |

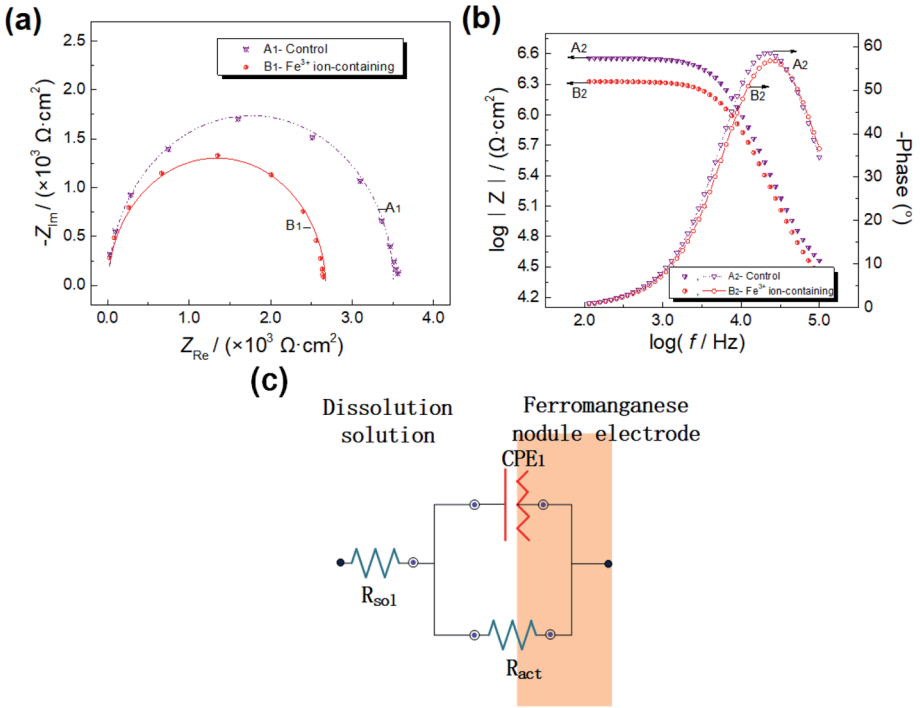


Fig. 7 Nyquist plots of the manganese nodule in various solutions: (a) Nyquist plots, (b) Bode plots, (c) fitting equivalent circuit, amplitude 5 mV, frequency 0.01–$10^5$ Hz, bias voltage OPC, pH 1.8, non $Fe^{3+}$ ion as control, $Fe^{3+}$ ion concentration of 1.0 g $L^{-1}$ as $Fe^{3+}$ ion-containing.

Table 3 Fitting results using the equivalent circuit (Fig. 7) for manganese nodule electrodes

| Simulated solution | $R_{sol}$/(Ω $cm^2$) | $\eta$ | CPE1 ($10^{-6}$ $\Omega^{-1}$ $cm^{-2}$ $s^{\eta}$) | $R_{act}$/ (Ω $cm^2$) |
|---|---|---|---|---|
| $Fe^{3+}$ ion-containing | 24.3 | 0.987 | 0.803 | 2671 |
| Control | 29.4 | 0.992 | 0.970 | 3512 |

results of the electrochemical measurements, it also can be concluded that the reduction leaching of manganese nodules is mainly controlled by the interfacial electrochemical reduction corresponding to manganese oxide, and the active conversion of $Fe^{3+}/Fe^{2+}$ couple could affect the transformation of $Mn^{4+}$-oxide in the nodule.

As discussed above, $Fe^3$, the fundamental ion affects the reductive leaching of ferromanganese nodule in sulphuric acid solutions, and it can be interpreted based on two courses: the first is the acceleration generated by the transformation of the

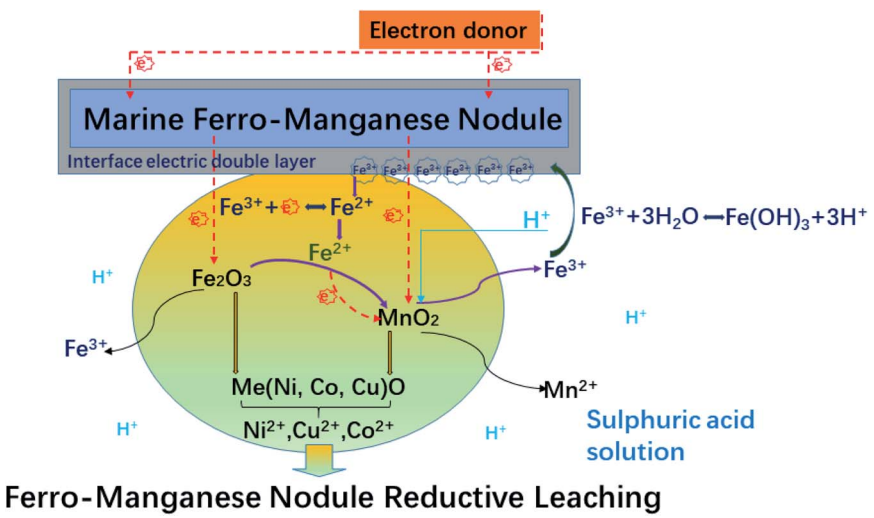


Fig. 8 Effects of $Fe^{3+}$ ions on manganese nodules reductive leaching in sulphuric acid solution.

$Fe^{3+}/Fe^{2+}$ pair, and the second is the hydrogen ion buffer action responding to $Fe^{3+}$ ion hydrolysis on the surface. Fig. 8 presents the probable roles of $Fe^{3+}$ ions on the manganese nodule reduction leaching in the sulphuric acid system.

## 4. Conclusions

The reductive leaching of ocean manganese nodule in sulphuric acid solution is mainly presented in two courses, an interface electrochemical reduction of Fe–Mn oxides and an acid dissolution of metal oxides, it is much depended on the reductive failure of the crystal structure of Mn–Fe oxides, and it is principally under the control of the reductive dissolution of high valence manganese oxide.

$Fe^{3+}$ ions, as fundamental ions leaching into lixivium, have beneficial effects on the reductive leaching of manganese nodules in the sulphuric acid solution with limits. The simulated leaching performance of the manganese nodule shows that $Fe^{3+}$ ion could facilitate metal extraction efficiencies under different pH values and $Fe^{3+}$ ion concentration conditions. According to the results of the leaching test and electrochemical analysis, $Fe^{3+}$ ion hydrolysis leads to a compensation of free hydrogen ion on the surface, which positively affects high valence manganese oxide reduction. On the other hand, the presence of $Fe^{3+}$ ions promotes the electrochemical transformations of manganese oxide. The results of electrochemical measurements present that $Fe^{3+}$ ions could accelerate the charge transfer of manganese oxide reduction dissolution in the sulphuric acid leaching system, due to the high-activity conversion of the $Fe^{3+}/Fe^{2+}$ redox couple and the underlying reduced trends of high valence manganese oxide.

## Author contributions

Kang Jin-xing: writing-original draft preparation, conceptualization, investigation, methodology. Wang Ya-yun: investigation; software. Qiu Yun-fei: writing-reviewing and editing, formal analysis, visualization.

## Conflicts of interest

There are no conflicts to declare.

## Acknowledgements

This study was supported by 'China Ocean Biological Resources Development Program (DY135-B2-15)'.

## References

1 K. Mizell and J. R. Hein, Ocean Floor Manganese Deposits, in *Encyclopedia of Geology*, Elsevier, 2021.
2 O. Sparenberg, A historical perspective on deep-sea mining for manganese nodule, 1965–2019, *The Extractive Industries and Society*, 2019, **6**(3), 842–854.
3 X.-f. Shi, Y.-z. Fu, B. Li, *et al.*, Research on deep-sea minerals in China: progress and discovery (2011-2020), *Bull. Mineral., Petrol. Geochem.*, 2021, **2**(40), 305–318.
4 J. L. Mero, Ocean-floor manganese nodule, *Econ. Geol.*, 1962, **57**(5), 747–767.
5 G. N. Baturin, *The geochemistry of manganese and manganese nodule in the ocean*, D. Reidel Pub. Co., 1988.
6 O. S. Vere Shchagin, E. N. Perova, A. I. Brusnitsyn, *et al.*, Ferro-manganese nodule from the Kara Sea: mineralogy, geochemistry and genesis, *Ore Geol. Rev.*, 2019, **106**, 192–204.
7 P. P. Sujith and M. Gonsalves, Ferromanganese oxide deposits: geochemical and microbiological perspectives of interactions of cobalt and nickel, *Ore Geol. Rev.*, 2021, **139**(11), 104458.
8 G. Senanayake, Acid leaching of metal from deep-sea manganese nodule – a critical review of fundamentals and applications, *Miner. Eng.*, 2011, **24**(13), 1379–1396.
9 F. Beolchini, A. Becci, G. Barone, *et al.*, High fungal-mediated leaching efficiency of valuable metal from deep-sea polymetallic nodule, *Environ. Technol. Innovation*, 2020, **20**, 101037.
10 W. Lei, Studies on Chemical Status of Manganese Nodule by a Selectively-Leaching Technique, *J. Xiamen Univ., Nat. Sci.*, 1989, **28**(3), 297–300.
11 M. Kawahara, K. Tokikawa and T. Mitsuo, Sulfating Roasting of Manganese Nodule and Selective Leaching of Roasted Ore, *Shigen to Sozai*, 1992, **107**(5), 305–309.
12 R. K. Jana and D. D. Akerkar, Studies of the metal-ammonia-carbon dioxide-water system in extraction metallurgy of polymetallic sea nodule, *Hydrometallurgy*, 1989, **22**(3), 363–378.
13 S. B. Kanungo, Rate process of the reduction leaching of manganese nodule in dilute HCl in presence of pyrite: part II: leaching behaviour of manganese, *Hydrometallurgy*, 1999, **52**(3), 331–347.
14 M. K. Ghosh, S. P. Barik and S. Anand, Sulphuric acid leaching of polymetallic nodule using paper as a reductant, *Trans. Indian Inst. Met.*, 2008, **61**(6), 477–481.
15 R. P. Das and S. Anand, *Metallurgical Processing of Polymetallic Ocean Nodule*, Springer International Publishing, 2017.
16 S. Ghosh, S. Mohanty, A. Akcil, *et al.*, A greener approach for resource recycling: manganese bioleaching, *Chemosphere*, 2016, **154**, 628–639.
17 C. Geng, B. Cja, B. Rla, *et al.*, Leaching kinetics of manganese from pyrolusite using pyrite as a reductant under microwave heating, *Sep. Purif. Technol.*, 2021, **277**, 119472.
18 H. Su, Y. Wen, W. Fan, *et al.*, Reductive leaching of manganese from low-grade manganese ore in $H_2SO_4$ using cane molasses as reductant, *Hydrometallurgy*, 2008, **93**(3–4), 136–139.
19 J. Ju, Y. Feng, H. Li, *et al.*, The limiting effect of manganese phase of oceanic cobalt-rich crust reduction by sawdust in acid leaching, *Sustainable Chem. Pharm.*, 2021, **19**(5), 100346.
20 M. K. Sinha, W. Purcell and W. Westhuizen, Recovery of manganese from ferruginous manganese ore using

ascorbic acid as reducing agent, *Miner. Eng.*, 2020, **154**, 106406.

21 C. Y. Wang, D. F. Qiu, F. Yin, *et al.*, Slurry electrolysis of ocean polymetallic nodule, *Trans. Nonferrous Met. Soc. China*, 2010, **20**, 60–64.

22 H. Vu, Leaching of manganese deep ocean nodule in $FeSO_4$–$H_2SO_4$–$H_2O$ solutions, *Hydrometallurgy*, 2005, **77**(1), 147–153.

23 E. Padhan, K. Sarangi and T. Subbaiah, Recovery of manganese and nickel from polymetallic manganese nodule using commercial extractants, *Int. J. Miner. Process.*, 2014, **126**, 55–61.

24 J.-x. Kang, Y.-l. Feng, H.-r. Li, *et al.*, New understanding of the reduction mechanism of pyrolusite in the *Acidithiobacillus ferrooxidans* bio-leaching system, *Electrochim. Acta*, 2019, **297**, 443–451.

25 A. Kumari and K. A. Natarajan, Development of a clean bioelectrochemical process for leaching of ocean manganese nodule, *Miner. Eng.*, 2002, **15**(1), 103–106.

26 J. X. Kang, Y. L. Feng, H. R. Li, *et al.*, Electrochemical Behaviour of Ocean Polymetallic Nodule and Low-Grade Nickel Sulphide Ore in *Acidithiobacillus ferrooxidans*-Coupled Bio-Leaching, *Minerals*, 2019, **9**(2), 1–20.

27 V. Inglezakis and M. Loizidou, Ion exchange of $Pb^{2+}$, $Cu^{2+}$, $Fe^{3+}$, and $Cr^{3+}$ on natural clinoptilolite: selectivity determination and influence of acidity on metal uptake, *J. Colloid Interface Sci.*, 2003, **261**(1), 49–54.

28 Y. Chabre and J. Pannetier, Structural and electrochemical properties of the proton/γ-$MnO_2$ system, *Prog. Solid State Chem.*, 1995, **23**(1), 1–130.

29 S. Karimi, A. Ghahreman and F. Rashchi, Kinetics of Fe(III)-Fe(II) redox half-reactions on sphalerite surface, *Electrochim. Acta*, 2018, **281**, 624–637.

30 D. Balachandran, D. Morgan and G. Ceder, First Principles Study of H-Insertion in $MnO_2$, *J. Solid State Chem.*, 2002, **166**(1), 91–103.

31 X. Liu, Y. Zhang, Y. He, *et al.*, Investigation of current oscillatory phenomena based on $Fe^{3+}/Fe^{2+}$ at the liquid/liquid interface, *J. Electroanal. Chem.*, 2012, **671**, 1–6.

32 G. H. Bochmann and W. Vielstich, On the reaction rate of the $Fe^{2+}/Fe^{3+}$ redox couple in sulfate solution, *Electrochim. Acta*, 1988, **33**, 805–809.